

Cross-validation based adaptive sampling for Gaussian process models

Hossein Mohammadi ^{*1, 2}, Peter Challenor^{1, 2}, Daniel Williamson¹, and Marc Goodfellow^{1, 2}

¹College of Engineering, Mathematics and Physical Sciences, University of Exeter, Exeter, UK

²EPSRC Centre for Predictive Modelling in Healthcare, University of Exeter, Exeter, UK

Abstract

In many real-world applications, we are interested in approximating black-box, costly functions as accurately as possible with the smallest number of function evaluations. A complex computer code is an example of such a function. In this work, a Gaussian process (GP) emulator is used to approximate the output of complex computer code. We consider the problem of extending an initial experiment (set of model runs) sequentially to improve the emulator. A sequential sampling approach based on leave-one-out (LOO) cross-validation is proposed that can be easily extended to a batch mode. This is a desirable property since it saves the user time when parallel computing is available. After fitting a GP to training data points, the expected squared LOO error (ESE_{LOO}) is calculated at each design point. ESE_{LOO} is used as a measure to identify important data points. More precisely, when this quantity is large at a point it means that the quality of prediction depends a great deal on that point and adding more samples in the nearby region could improve the accuracy of the GP model. As a result, it is reasonable to select the next sample where ESE_{LOO} is maximum. However, such quantity is only known at the experimental design and needs to be estimated at unobserved points. To do this, a second GP is fitted to the ESE_{LOO} s and where the maximum of the modified expected improvement (EI) criterion occurs is chosen as the next sample. EI is a popular acquisition function in Bayesian optimisation and is used to trade-off between local/global search. However, it has tendency towards exploitation, meaning that its maximum is close to the (current) “best” sample. To avoid clustering, a modified version of EI, called pseudo expected improvement, is employed which is more explorative than EI and allows us to discover unexplored regions. The results show that the proposed sampling method is promising.

*Corresponding Author: h.mohammadi@exeter.ac.uk

Keywords: Adaptive sampling; Computer experiment; Leave-one-out cross-validation; Gaussian processes

1 Introduction

In many real-world applications, we are interested in predicting the output of complex computer models (or simulators) such as high fidelity numerical solvers. The reason is that such models are computationally intensive and we cannot use them to perform analysis that requires very many runs. One way to predict the model output is to use surrogate models which are constructed based on a limited number of simulation runs. Surrogates are fast to run and the analysis can be carried out on them, see e.g. [27, 46, 2]. Among different classes of surrogate models, Gaussian process (GP) emulators [38] have gained increasing attention due to their statistical properties such as computational tractability and flexibility. GPs provide a flexible paradigm to approximate any smooth, continuous function [33] thanks to the variety of covariance kernels available. Most importantly, the GP prediction is equipped with an estimation of uncertainty which reflects the accuracy of the prediction.

One factor that heavily affects the accuracy of emulators is the locations of the training data, also called design or sample points, [45, 21]. The design of computer experiments (DoE) [40, 41] is a common way to select the samples within the input space. Generally speaking, this can be performed in a *one-shot* or *adaptive* manner [28]. In the former all samples are chosen at once while in the latter the points are selected sequentially using information from the emulator and the existing data. Examples of one-shot algorithms are the Latin hypercube [31], full factorial [6] and orthogonal array designs [34]. A potential drawback of one-shot DoEs is that they may result in under/oversampling [43, 12]. However, this is not the case of adaptive approaches where we can stop the sampling process, which is computationally expensive, as soon as the emulator reaches an acceptable level of accuracy. Moreover, with adaptive sampling it is possible to take more samples in “interesting” regions where e.g. the underlying function is highly nonlinear or exhibits abrupt changes. This paper focuses on GP-based adaptive sampling where an initial design is extended sequentially to improve the emulator. The initial DoE is often *space-filling* meaning that the points are scattered uniformly over the input space. We refer the reader to [37, 20] and references therein for more information on space-filling designs.

There are various GP-based adaptive sampling methods which can be categorised according to their selection criteria, i.e. the strategies to find future designs. The readers are referred to [12, 28] for a comprehensive review of the existing methods. An intuitive criterion is the built-in predictive variance of GPs, also known as the prediction uncertainty or mean squared error (MSE). The idea is that the predictive variance is regarded as an estimation of the “real” prediction error and a point with the maximum uncertainty is taken as the next experimental design [30, 17]. The predictive variance increases away

from the data points. It is highly probable that sampling based on the MSE criterion ends up some sort of space-filling design which can be achieved using one-shot techniques. Moreover, MSE is large on the boundaries of the input space that causes taking a lot of samples on the boundaries. However, this is not desirable in many situations especially when the main characteristics of the true function appear inside the interior region. The integrated mean square error (IMSE) is a variant of the MSE criterion and selects a new point if adding that point to the existing design minimises the integral of MSE [40, 35]. However, computing IMSE is cumbersome especially in high dimensions.

The maximum entropy measure is another criterion employed in the framework of the GP-based adaptive sampling [44, 22]. It is shown that the maximum entropy and maximum MSE criteria are equivalent [17, 24]. Thus, an adaptive sampling strategy based on the maximum entropy measure tends to place many points at the borders of the input space [22]. This issue can be tackled using the mutual information criterion [8, 3]. However, this method is not easy to implement and maximising mutual information is an NP-hard problem [23].

The leave-one-out (LOO) cross-validation error defines another class of adaptive sampling criterion [26, 25, 1, 29]. To obtain the LOO error at an experimental design we remove that point from the training data set. Then, a GP is fitted to the remaining samples and the response at the left out point is predicted. The difference between the predicted and actual response serves as the LOO error. A relatively small error indicates that the prediction accuracy in a vicinity of the removed point is high and there is good information about the true function there. On the other hand, a comparably large error means that the removed point has a huge impact on the accuracy of the emulator and hence, we need more samples in the nearby region to reduce the errors. In [47] scores obtained by cross-validation are used to identify regions of distinct model behaviour and specify mixture of covariance functions for GP emulators. Using the LOO errors as sampling criterion has several advantages. First, it provides actual prediction error at the design points. Second, it is model-independent and can be achieved by any surrogate model. For example, in [5] a methodology based on the LOO cross-validation is proposed to estimate the prediction uncertainty of any surrogate model, either deterministic or probabilistic. Third, computing the LOO errors is not expensive in terms of computational cost [9]. However, the LOO errors are not determined everywhere in the input space and only defined at locations where we have pre-existing model runs.

This paper proposes an adaptive sampling DoE relying on the LOO cross-validation method to build GP emulators as accurately as possible for deterministic computer codes over the entire domain. The proposed method has a few parameters to be tuned and can be extended to a batch mode where at each iteration a set of inputs is selected for evaluation. This is an important property as it saves the user time when parallel computing is available [48]. The remainder of the paper is organised as follows. In the next section, the statistical methodology of GP emulators is briefly reviewed. Section 3 introduces the proposed adaptive sampling approach and its extension to the batch mode. Section

4 presents numerical experiments where the predictive performance of our algorithm is tested. Finally, the paper’s conclusion is in Section 5.

2 Gaussian process models

First we look at GP emulators and their statistical background. Let the underlying function of a deterministic complex computer code is given by $f : \mathcal{D} \mapsto \mathbb{R}$ in which \mathcal{D} is a compact set in \mathbb{R}^d . Suppose $\mathcal{A} = \{\mathbf{X}_n, \mathbf{y}_n\}$ is a training data set where $\mathbf{X}_n = (\mathbf{x}_1, \dots, \mathbf{x}_n)^\top$ and $\mathbf{y}_n = (f(\mathbf{x}_1), \dots, f(\mathbf{x}_n))^\top$ represent n locations in the input space \mathcal{D} and the corresponding outputs (responses/observations), respectively. To approximate f , we model \mathbf{y}_n as a Gaussian process $(Z_0(\mathbf{x}))_{\mathbf{x} \in \mathcal{D}}$ whose mean and covariance function are defined as

$$m_0 : \mathcal{D} \mapsto \mathbb{R} ; m_0(\mathbf{x}) = \mathbb{E}[Z_0(\mathbf{x})] \quad (1)$$

$$k_0 : \mathcal{D} \times \mathcal{D} \mapsto \mathbb{R} ; k_0(\mathbf{x}, \mathbf{x}') = \text{Cov}(Z_0(\mathbf{x}), Z_0(\mathbf{x}')) . \quad (2)$$

In this framework, $Z_0(\mathbf{x})$ is regarded as a random function such that for any finite set of inputs, the associated outputs have the multivariate Gaussian distribution [38]. Without loss of generality, we assume that the GP mean is a constant function given by $m_0(\mathbf{x}) = \mu$. The positive semi-definite covariance function k_0 plays an important role in GP modelling; assumptions about the underlying function such as differentiability or periodicity are encoded through kernels. The Matérn family of kernels are commonplace in computer experiments and (in the univariate case) are defined as

$$k_0(x, x') = \sigma^2 \frac{2^{1-\nu}}{\Gamma(\nu)} \left(\frac{\sqrt{2\nu}}{\theta} |x - x'| \right)^\nu B_\nu \left(\frac{\sqrt{2\nu}}{\theta} |x - x'| \right), \quad (3)$$

where $\Gamma(\cdot)$ is the Gamma function and $B_\nu(\cdot)$ denotes the modified Bessel function of the second kind of order ν . The parameter ν regulates the degree of smoothness of the GP sample paths/functions such that a process with the Matérn kernel of order ν is $\lfloor \nu - 1 \rfloor$ times differentiable. The positive parameters σ^2 and θ are referred to as the *process variance* and *correlation length scale*, respectively. These parameters are usually unknown and need to be estimated from data. We refer the reader to [18, 38, 13] for a more detailed explanation on parameter estimation techniques.

The GP prediction is obtained by conditioning it on the observations:

$$Z_n(\mathbf{x}) = Z_0(\mathbf{x}) \mid \mathbf{y}_n = Z_0(\mathbf{x}) \mid Z_0(\mathbf{x}_1) = f(\mathbf{x}_1), \dots, Z_0(\mathbf{x}_n) = f(\mathbf{x}_n).$$

The conditional mean, $m_n(\mathbf{x}) = \mathbb{E}[Z_n(\mathbf{x})]$, and covariance, $k_n(\mathbf{x}, \mathbf{x}') = \text{Cov}(Z_n(\mathbf{x}), Z_n(\mathbf{x}'))$,

have closed-form expressions as [38]

$$m_n(\mathbf{x}) = \hat{\mu} + \mathbf{k}(\mathbf{x})^\top \mathbf{K}^{-1}(\mathbf{y}_n - \hat{\mu}\mathbf{1}) \quad (4)$$

$$k_n(\mathbf{x}, \mathbf{x}') = k_0(\mathbf{x}, \mathbf{x}') - \mathbf{k}(\mathbf{x})^\top \mathbf{K}^{-1} \mathbf{k}(\mathbf{x}') + \frac{(1 - \mathbf{1}^\top \mathbf{K}^{-1} \mathbf{k}(\mathbf{x})) (1 - \mathbf{1}^\top \mathbf{K}^{-1} \mathbf{k}(\mathbf{x}'))}{\mathbf{1}^\top \mathbf{K}^{-1} \mathbf{1}}, \quad (5)$$

given that all unknown parameters are estimated. Here, $\mathbf{k}(\mathbf{x}) = (k_0(\mathbf{x}, \mathbf{x}_1), \dots, k_0(\mathbf{x}, \mathbf{x}_n))^\top$ is the vector of covariances between $Z_0(\mathbf{x})$ and $Z_0(\mathbf{x}_i)$ s, $\mathbf{1}$ is a vector of ones and \mathbf{K} is an $n \times n$ covariance matrix with elements $\mathbf{K}_{ij} = k_0(\mathbf{x}_i, \mathbf{x}_j)$, $\forall 1 \leq i, j \leq n$. The conditional variance $s_n^2(\mathbf{x}) = k_n(\mathbf{x}, \mathbf{x})$ determines the uncertainty associated with the prediction at $\mathbf{x} \in \mathcal{D}$ and is a measure of the prediction accuracy. In adaptive sampling based on the MSE criterion, the new sample is the point that maximises $s_n^2(\mathbf{x})$.

3 Proposed adaptive sampling method

Before introducing our method, it is worth mentioning that an “efficient” adaptive sampling strategy should meet the conditions below [28].

- (i) **Local exploitation:** that allows us to add more points in interesting areas discovered so far.
- (ii) **Global exploration:** by which unexplored domain regions can be detected.
- (iii) **Trade off between local exploitation and global exploration:** which balances the previous two objectives using a suitable measure.

The proposed adaptive sampling approach uses *expected squared LOO error*, see Section 3.1, for local exploitation. The global exploration and the trade off between the local/global search is driven by the *pseudo expected improvement* criterion introduced in Section 3.2.

3.1 Expected squared LOO cross-validation error

We wish to improve the GP emulator $Z_n(\mathbf{x})$ constructed on the training data set \mathcal{A} using the LOO cross-validation method. To do so, the first step is to obtain the LOO errors. Let $e_{LOO}(\mathbf{x}_i)$ denote the LOO cross-validation error at the design site \mathbf{x}_i , $1 \leq i \leq n$. The computation of $e_{LOO}(\mathbf{x}_i)$ relies on the Gaussian process $Z_{n,-i}(\mathbf{x})$ which is obtained by conditioning $Z_0(\mathbf{x})$ on all observations except the i -th one: $Z_{n,-i}(\mathbf{x}) = Z_0(\mathbf{x}) \mid \mathbf{y}_n \setminus \{f(\mathbf{x}_i)\}$. The conditional mean and variance of $Z_{n,-i}(\mathbf{x})$ are shown by $m_{n,-i}(\mathbf{x})$ and $s_{n,-i}^2(\mathbf{x})$, respectively. The LOO cross-validation error is then calculated as

$$e_{LOO}(\mathbf{x}_i) = |m_{n,-i}(\mathbf{x}_i) - f(\mathbf{x}_i)|, \quad (6)$$

which can be regarded as the sensitivity of the emulator to the left out point \mathbf{x}_i . As a result, the idea of adding new samples near the points with large LOO errors is used in several adaptive sampling works, see e.g. [26, 1]. In this work, we use the estimated parameters of $Z_n(\mathbf{x})$ to build $Z_{n,-i}(\mathbf{x})$ and do not re-estimate them in order to alleviate the computational burden. Moreover, Equation (6) can be calculated efficiently using the formula proposed in [9].

The LOO error $e_{LOO}(\mathbf{x}_i)$ only accounts for the difference between the predictive mean and the real value at \mathbf{x}_i and can be a misleading selection criterion in some situations. Figure 1 shows an example where the prediction at $x_5 = 0$ is equal to the true value there and therefore $e_{LOO}(x_5) = 0$. This means that the chance of adding a new sample near the fifth data point is low although it is in a crucial region. The above mentioned problem can be mitigated using “expected squared LOO error (ESE_{LOO})” which provides more information than the LOO error about the sensitivity of the emulator to the design points. More precisely, ESE_{LOO} accounts for both the prediction uncertainty and the difference between the prediction and the true value, see the next paragraph.

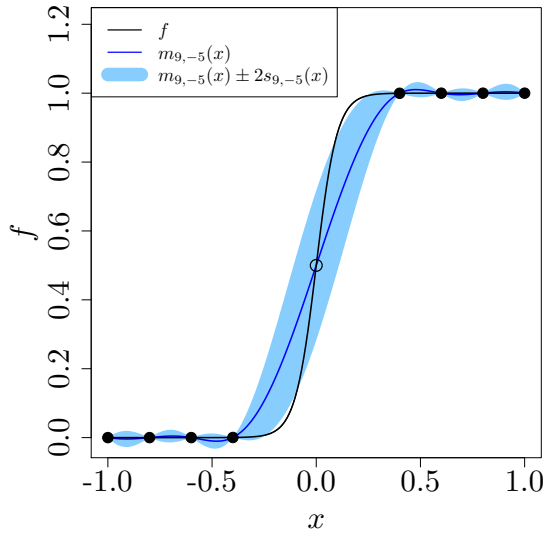


Figure 1: The LOO error (Equation (6)) can be misleading as a selection criterion. Removing the fifth sample, i.e. $(0, 0.5)$, does not change the prediction at $x = 0$ and the LOO error remains zero there: $|m_{g,-5}(x_5) - f(x_5)| = 0$. This means that the point $(0, 0.5)$ does not have any influence on the emulator while f has a large gradient there. However, the expected squared LOO error which accounts for the prediction uncertainty is not zero at x_5 . The true function is $f(x) = \frac{1}{1+\exp(-20x)}$.

The expected squared LOO error at the design site \mathbf{x}_i is defined as

$$ESE_{LOO}(\mathbf{x}_i) = \frac{\mathbb{E} \left[(Z_{n,-i}(\mathbf{x}_i) - f(\mathbf{x}_i))^2 \right]}{\sqrt{\text{Var} \left((Z_{n,-i}(\mathbf{x}_i) - f(\mathbf{x}_i))^2 \right)}}, \quad (7)$$

in which the numerator and denominator (as normalisation factor) take the forms of

$$\mathbb{E} \left[(Z_{n,-i}(\mathbf{x}_i) - f(\mathbf{x}_i))^2 \right] = s_{n,-i}^2(\mathbf{x}_i) + (m_{n,-i}(\mathbf{x}_i) - f(\mathbf{x}_i))^2 \quad (8)$$

$$\text{Var} \left((Z_{n,-i}(\mathbf{x}_i) - f(\mathbf{x}_i))^2 \right) = 2s_{n,-i}^4(\mathbf{x}_i) + 4s_{n,-i}^2(\mathbf{x}_i) (m_{n,-i}(\mathbf{x}_i) - f(\mathbf{x}_i))^2. \quad (9)$$

To see how the above equations are obtained we first note that $Z_{n,-i}(\mathbf{x}_i)$ is a random normal variable (see Figure 2) specified by

$$Z_{n,-i}(\mathbf{x}_i) \sim \mathcal{N} \left(m_{n,-i}(\mathbf{x}_i), s_{n,-i}^2(\mathbf{x}_i) \right), \quad (10)$$

according to the GP definition. By subtracting $f(\mathbf{x}_i)$ from both sides of (10) and dividing them by $s_{n,-i}(\mathbf{x}_i)$ we reach

$$\frac{Z_{n,-i}(\mathbf{x}_i) - f(\mathbf{x}_i)}{s_{n,-i}(\mathbf{x}_i)} \sim \mathcal{N} \left(\frac{m_{n,-i}(\mathbf{x}_i) - f(\mathbf{x}_i)}{s_{n,-i}(\mathbf{x}_i)}, 1 \right), \quad (11)$$

in which the square of the left hand side is a random variable with noncentral chi-square distribution characterised by

$$\left(\frac{Z_{n,-i}(\mathbf{x}_i) - f(\mathbf{x}_i)}{s_{n,-i}(\mathbf{x}_i)} \right)^2 \sim \chi'^2 \left(\kappa = 1, \lambda = \left(\frac{m_{n,-i}(\mathbf{x}_i) - f(\mathbf{x}_i)}{s_{n,-i}(\mathbf{x}_i)} \right)^2 \right). \quad (12)$$

Here, κ and λ are the degrees of freedom and noncentrality parameter, respectively¹. As a result

$$\mathbb{E} \left[\left(\frac{Z_{n,-i}(\mathbf{x}_i) - f(\mathbf{x}_i)}{s_{n,-i}(\mathbf{x}_i)} \right)^2 \right] = 1 + \left(\frac{m_{n,-i}(\mathbf{x}_i) - f(\mathbf{x}_i)}{s_{n,-i}(\mathbf{x}_i)} \right)^2, \quad (13)$$

$$\text{Var} \left(\left(\frac{Z_{n,-i}(\mathbf{x}_i) - f(\mathbf{x}_i)}{s_{n,-i}(\mathbf{x}_i)} \right)^2 \right) = 2 \left(1 + 2 \left(\frac{m_{n,-i}(\mathbf{x}_i) - f(\mathbf{x}_i)}{s_{n,-i}(\mathbf{x}_i)} \right)^2 \right). \quad (14)$$

Finally, if the expectation and variance in the above equations are multiplied by $s_{n,-i}^2(\mathbf{x}_i)$, we reach Equations (8) and (9).

¹Suppose X_1, \dots, X_κ are κ independent random normal variables such that $X_i \sim \mathcal{N}(\mu_i, 1)$, $1 \leq i \leq \kappa$. Then, $\sum_{i=1}^{\kappa} X_i^2 \sim \chi'^2(\kappa, \lambda = \sum_{i=1}^{\kappa} \mu_i^2)$ has a noncentral chi-square distribution with mean $\kappa + \lambda$ and variance $2(\kappa + 2\lambda)$.

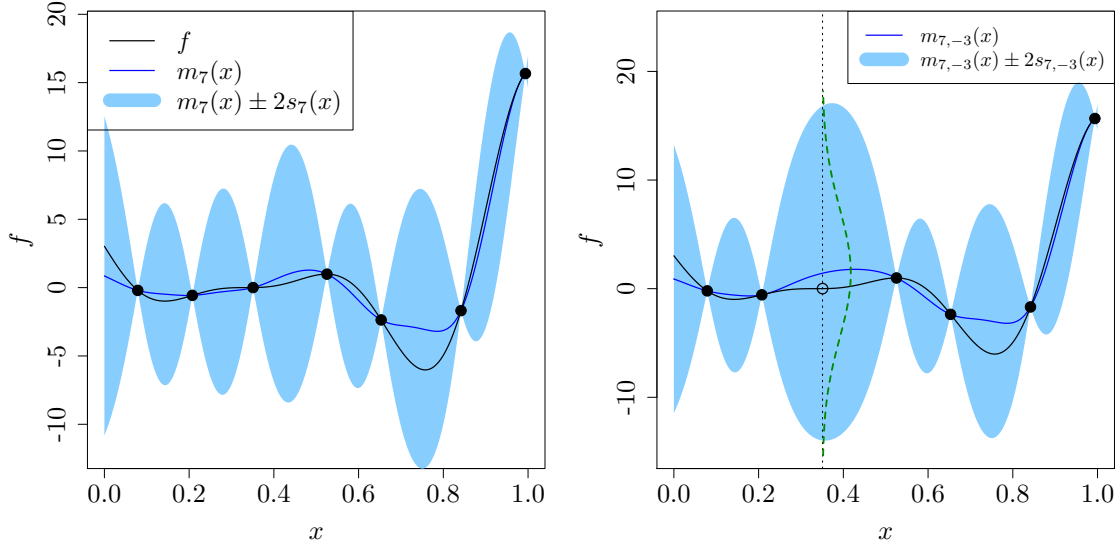


Figure 2: Left: Gaussian process prediction (blue) with 95% credible intervals (shaded) based on 7 observations from the true function (black). Right: GP prediction based on the training data except the third one where the GP has a normal distribution specified by Equation (10).

The analytical expression of Equation (8) is similar to the *expected improvement for global fit (EIGF)* infill sampling criterion proposed by Lam [24]. In Section 4, we compare the predictive performance of our method with EIGF on several test functions. In EIGF, the improvement at an arbitrary point \mathbf{x} is given by:

$$IGF(\mathbf{x}) = (Z_n(\mathbf{x}) - f(\mathbf{x}_i^*))^2, \quad (15)$$

where $f(\mathbf{x}_i^*)$ is the response at the location \mathbf{x}_i^* which is closest (in Euclidean distance) to \mathbf{x} . The EIGF criterion is the expected value of $IGF(\mathbf{x})$ and takes the following form

$$EIGF(\mathbf{x}) = \mathbb{E}[IGF(\mathbf{x})] = (m_n(\mathbf{x}) - f(\mathbf{x}_i^*))^2 + s_n^2(\mathbf{x}). \quad (16)$$

Using EIGF as the selection criterion, the next sample is chosen where EIGF is maximum:

$$\mathbf{x}_{n+1} = \operatorname{argmax}_{\mathbf{x} \in \mathcal{D}} EIGF(\mathbf{x}).$$

3.2 Proposed selection criterion

Since the magnitude of $ESE_{LOO}(\mathbf{x}_i)$ reflects the sensitivity of the emulator to the loss of information provided by the function evaluation at \mathbf{x}_i , it is reasonable to choose the next

sample where ESE_{LOO} is maximum. However, this quantity is only defined at the training data while we need to find the maximum of ESE_{LOO} over the whole domain. One way around this problem is to estimate ESE_{LOO} at unobserved locations via surrogate models. In this work, we use a second GP emulator to estimate $ESE_{LOO}(\mathbf{x})$ where $\mathbf{x} \in \mathcal{D}$ is a generic location. The training set for the second GP model, denoted by $Z_n^e(\mathbf{x})$, is $\{\mathbf{X}_n, \mathbf{y}_n^e\}$ such that $\mathbf{y}_n^e = (ESE_{LOO}(\mathbf{x}_1), \dots, ESE_{LOO}(\mathbf{x}_n))^T$. The (conditional) mean and variance of $Z_n^e(\mathbf{x})$ are indicated by $m_n^e(\mathbf{x})$ and $s_n^e(\mathbf{x})$, respectively.

After estimating $ESE_{LOO}(\mathbf{x})$, we can find its maximum applying techniques in surrogate-based optimisation. In this framework, a naive approach is to maximise $m_n^e(\mathbf{x})$. However, this simple strategy does not define a valid optimisation scheme due to *overexploitation* [18] meaning that the new samples are taken very close to the points with large ESE_{LOO} . To overcome this problem, we need to take into account $s_n^e(\mathbf{x})$ as the exploration component in the course of search. To this end, we employ *Expected improvement (EI)* which is one of the most common acquisition functions in Bayesian optimisation [7, 18] to trade-off between exploration and exploitation. It is expressed by

$$EI(\mathbf{x}) = \begin{cases} (m_n^e(\mathbf{x}) - \max(\mathbf{y}_n^e)) \Phi(u) + s_n^e(\mathbf{x}) \phi(u) & \text{if } s_n^e(\mathbf{x}) > 0 \\ 0 & \text{if } s_n^e(\mathbf{x}) = 0, \end{cases} \quad (17)$$

where $u = \frac{m_n^e(\mathbf{x}) - \max(\mathbf{y}_n^e)}{s_n^e(\mathbf{x})}$, $\phi(\cdot)$ and $\Phi(\cdot)$ represent the PDF and CDF of the standard normal distribution, respectively. EI is a non-negative, parameter-free function and is null at the data points. However, it is shown that EI is bias towards exploitation especially at the beginning of the search [42, 19, 36]. As a result, if EI is used to find the maximum of $ESE_{LOO}(\mathbf{x})$ at each iteration, clustering happens. This is illustrated by an example in Figure 3. In this paper, *pseudo expected improvement (PEI)* [49] is considered as the selection criterion which has a better exploration property than EI. Pseudo expected improvement is obtained by multiplying EI by a repulsive function (RF): $PEI(\mathbf{x}) = EI(\mathbf{x})RF(\mathbf{x})$, see Figure 4. The repulsive function is defined as

$$RF(\mathbf{x}; \mathbf{X}_n) = \prod_{i=1}^n [1 - \text{Corr}(Z_n^e(\mathbf{x}), Z_n^e(\mathbf{x}_i))], \quad (18)$$

where $\text{Corr}(\cdot, \cdot)$ is the correlation function of $Z_n^e(\cdot)$. $RF(\mathbf{x})$ is a measure of the (canonical) distance between \mathbf{x} and the designs; it is always between zero and one and null at the data points because $\text{Corr}(Z_n^e(\mathbf{x}_i), Z_n^e(\mathbf{x}_i)) = 1, \forall \mathbf{x}_i \in \mathbf{X}_n$.

The correlation function in Equation (18) depends on length-scales $\boldsymbol{\theta}^e = [\theta_1^e, \dots, \theta_d^e]^T$ that are estimated from $\{\mathbf{X}_n, \mathbf{y}_n^e\}$. It is important that θ_i^e s do not take very ‘‘small’’ values to circumvent clustering. The reason is that when they come near zero, $\text{Corr}(Z_n^e(\mathbf{x}), Z_n^e(\mathbf{x}_i))$ tends to zero and $RF(\mathbf{x})$ is (almost) one everywhere meaning that it has no influence on EI. Besides, the maximum of EI is located in a shrinking neighbourhood of the current best point when $\boldsymbol{\theta}^e$ is small [32]. Therefore, a lower bound has to be considered for $\boldsymbol{\theta}^e$. In

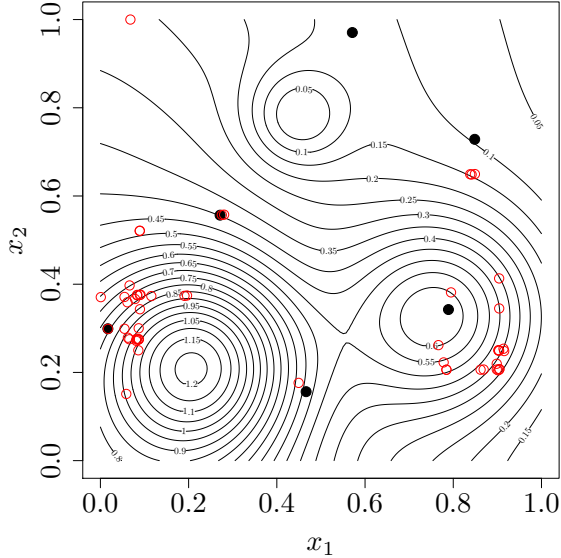


Figure 3: Adaptive designs (red circles) are obtained by maximising $ESE_{LOO}(\mathbf{x})$ using the EI criterion. The filled circles are the initial DoE and the true function is Franke’s function, see Section 4. EI tends towards exploitation and as a result clustering occurs.

a normalised input space, i.e. $\mathcal{D} = [0, 1]^d$, we define this lower bound to be

$$\theta_{lb}^e = \sqrt{-0.5 / \ln(10^{-8})}, \quad (19)$$

for each dimension. It is obtained by setting the minimum correlation equal to 10^{-8} for the squared exponential correlation function defined as

$$k_0(x, x') = \exp\left(-\frac{|x - x'|^2}{2\theta^2}\right). \quad (20)$$

In the above equation, the minimum correlation between x and x' happens when $|x - x'| = 1$ which is the maximum distance between the two points in the normalised input space.

A common issue in adaptive sampling strategies is that many design points lie along the boundaries of the input space. Such samples might be nonoptimal if the true model is not feasible on the boundaries [14]. However, this problem can be alleviated in our approach by introducing “pseudo points”, denoted by \mathbf{X}_p , at appropriate locations within the design space. Pseudo points are used to update the repulsive function, i.e. $RF(\mathbf{x}; \mathbf{X}_n \cup \mathbf{X}_p)$, but the true function is not evaluated there due to computational cost. The following locations are suggested as the pseudo points

1. corners of the input space,

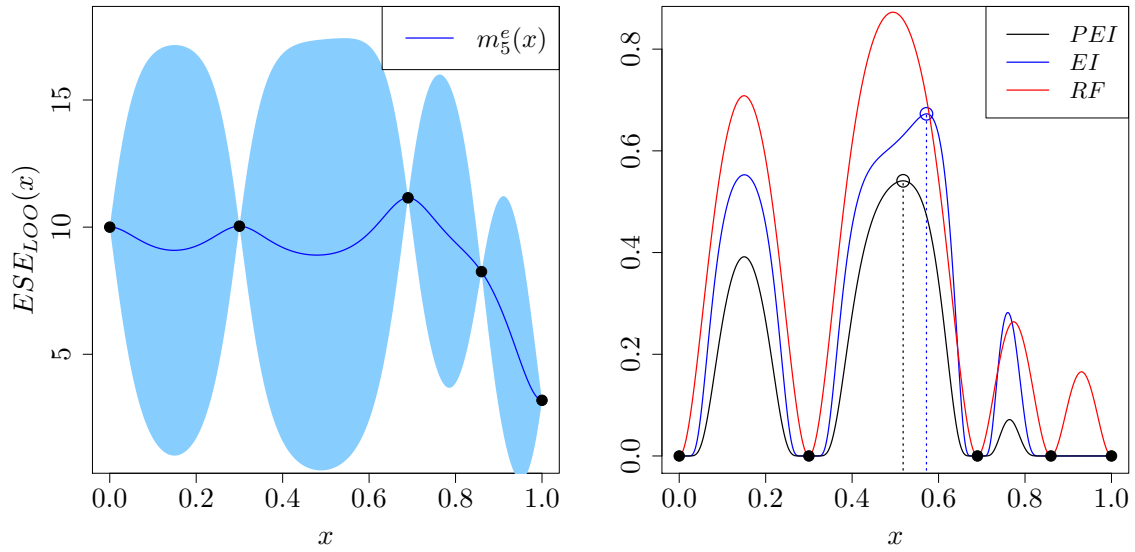


Figure 4: Left: A GP is fitted to five expected squared LOO errors. Right: Pseudo expected improvement (black) is obtained by multiplying expected improvement (blue) by the influence functions (red). The next sample point is where the PEI is maximum (black circle). The maximum of EI is shown by the blue circle. The PEI criterion is more explorative than EI.

2. closest point on each face of the (rectangular) input region to the initial DoE.

A 2-dimensional example is illustrated in Figure 5 that shows the location of pseudo points (red triangles) and six initial designs (black points). Finally, Algorithm 1 summarises the steps of the proposed adaptive sampling method.

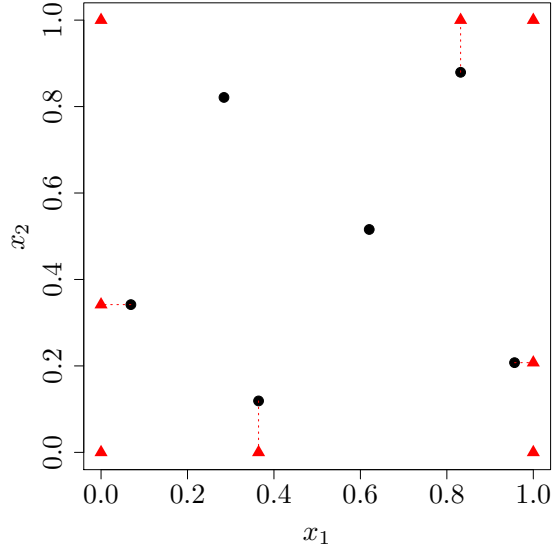


Figure 5: Initial DoE (black points) and pseudo points (red triangles). They are closest point on each face of the input space to the initial DoE and also at the corners of the region.

3.3 Extension to the batch mode

When parallel computing is available, it is preferred to evaluate the time-consuming function f in a set of inputs rather than a single point since it saves the user time. In batch sampling, $q > 1$ locations are chosen for evaluation at each iteration. Note that the computation time of running the simulator on q parallel cores is the same as a single run. The PEI criterion can be employed in a batch mode thanks to the repulsive function. In the sequel we show how to choose q points $\mathbf{x}_{n+1}, \dots, \mathbf{x}_{n+q}$ in a single iteration. The first point \mathbf{x}_{n+1} is obtained by maximising the PEI criterion. Then, the repulsive function is updated by \mathbf{x}_{n+1}

$$RF(\mathbf{x}; \mathbf{X}_n \cup \mathbf{x}_{n+1}) = \prod_{i=1}^{n+1} [1 - \text{Corr}(Z_n^e(\mathbf{x}), Z_n^e(\mathbf{x}_i))], \quad (21)$$

which updates PEI without evaluating f at \mathbf{x}_{n+1} . The second location \mathbf{x}_{n+2} is selected where the updated PEI is maximum. We repeat this procedure until the last point \mathbf{x}_{n+q}

Algorithm 1 Proposed sequential sampling approach

- 1: Create an initial design: $\mathbf{X}_n = \{\mathbf{x}_1, \dots, \mathbf{x}_n\}$
 - 2: Evaluate f at \mathbf{X}_n : $\mathbf{y}_n = f(\mathbf{X}_n)$
 - 3: Fit the Gaussian process $Z_n(\mathbf{x})$ to $\{\mathbf{X}_n, \mathbf{y}_n\}$
 - 4: **while not stop do**
 - 5: **for** $i = 1$ to n **do**
 - 6: Calculate $ESE_{LOO}(\mathbf{x}_i)$ using Equation (7)
 - 7: **end for**
 - 8: Set $\mathbf{y}_n^e = (ESE_{LOO}(\mathbf{x}_1), \dots, ESE_{LOO}(\mathbf{x}_n))^\top$
 - 9: Set the lower bound for θ^e using Equation (19)
 - 10: Fit $Z_n^e(\mathbf{x})$ to $\{\mathbf{X}_n, \mathbf{y}_n^e\}$
 - 11: Calculate $PEI(\mathbf{x}) = EI(\mathbf{x})RF(\mathbf{x})$
 - 12: $\mathbf{x}_{n+1} \leftarrow \arg\max PEI(\mathbf{x})$ and set $\mathbf{X}_n = \mathbf{X}_n \cup \{\mathbf{x}_{n+1}\}$
 - 13: $y_{n+1} \leftarrow f(\mathbf{x}_{n+1})$ and set $\mathbf{y}_n = \mathbf{y}_n \cup \{y_{n+1}\}$
 - 14: Update $Z_n(\mathbf{x})$ using the new data point $(\mathbf{x}_{n+1}, y_{n+1})$
 - 15: $n \leftarrow n + 1$
 - 16: **end while**
-

is chosen

$$RF(\mathbf{x}; \mathbf{X}_n \cup \mathbf{x}_{n+1} \cup \dots \cup \mathbf{x}_{n+q-1}) = \prod_{i=1}^{n+q-1} [1 - \text{Corr}(Z_n^e(\mathbf{x}), Z_n^e(\mathbf{x}_i))]$$
$$\mathbf{x}_{n+q} = \arg \max_{\mathbf{x} \in \mathcal{D}} EI(\mathbf{x}) RF(\mathbf{x}; \mathbf{X}_n \cup \mathbf{x}_{n+1} \cup \dots \cup \mathbf{x}_{n+q-1}).$$

Figure 6 shows our adaptive sampling method in the batch mode where $q = 3$ points are selected in one iteration.

4 Numerical experiments

Experimental results are presented and discussed in this section. Four analytic test functions and two real-world problems are considered as the “true” function to assess the efficiency of our proposed sampling method. The results are compared with other approaches including MSE, EIGF [24] and one-shot Latin hypercube sampling (LHS).

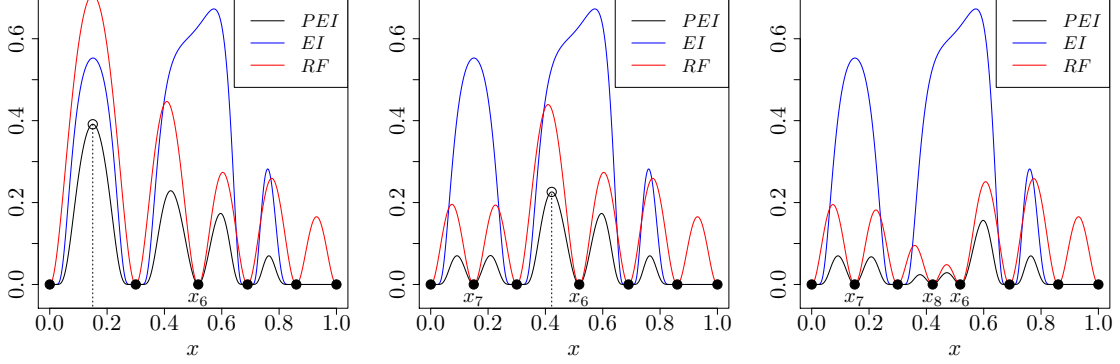


Figure 6: The process of selecting a batch of $q = 3$ points, x_{n+j} , $1 \leq j \leq 3$, where the size of initial DoE is $n = 5$. Left: the first query point, x_6 , is chosen where PEI is maximum. Middle: PEI is updated by multiplying the initial EI by $RF(x; x_{1:5} \cup x_6)$. The second query point, x_7 , is the location of maximum updated PEI. Right: PEI is updated using x_7 and the third sample, x_8 , is selected as explained.

4.1 Experimental setup

The prediction accuracy is assessed by the *root mean squared error (RMSE)* criterion. Given the test set $\{(\mathbf{x}_t, f(\mathbf{x}_t))\}_{t=1}^{t=N}$, RMSE is defined as

$$RMSE = \sqrt{\frac{\sum_{t=1}^N (m_n(\mathbf{x}_t) - f(\mathbf{x}_t))^2}{N}}, \quad (22)$$

which measures the distance between the emulator, $m_n(\mathbf{x}_t)$, and the true function, $f(\mathbf{x}_t)$. In our experiments, $N = 3000$ and the test points are selected uniformly across the input space. A total budget equal to $30d$ is considered for each experiment. The initial space-filling DoE is of size $3d$ and is obtained by the `maximinESE_LHS` function implemented in the R package `DiceDesign` [10]. There are ten different initial DoEs for every function and we assess the prediction performance of each method using all ten sets. The R package `DiceKriging` [39] is employed to construct GP models. The covariance kernel for modelling the true function and ESE_{LOO} is Matérn with $\nu = 3/2$. Since ESE_{LOO} is a positive quantity, the GP emulator is fitted to its natural logarithm.

4.2 Test functions

The four test functions are

- $f_1(\mathbf{x})$: Franke’s function [15], $d = 2$
- $f_2(\mathbf{x})$: Hartman function [16], $d = 3$

- $f_3(\mathbf{x})$: Friedman function [11], $d = 5$
- $f_4(\mathbf{x})$: Gramacy & Lee function [14], $d = 6$

and their analytic expression are given in Appendix A. Figure 7 illustrates the prediction performance of our proposed method ESE_{LOO} : sequential (black) and batch with $q = 4$ (orange), MSE (blue) and EIGF (red). Each curve represents the median of ten RMSEs using ten different initial DoEs. The x -axis shows the number of function evaluations divided by the problem dimension, d . The y -axis is on logarithmic scale. The dashed grey lines are the median of RMSEs based on one-shot LHS of sizes (from top to bottom): $10d$, $20d$ and $30d$, respectively.

Generally, the prediction performance of our method is comparable to other approaches. In particular, it outperforms MSE and EIGF in approximating the Hartman (f_2) and Gramacy & Lee (f_4) functions. The sequential (black) and batch (orange) ESE_{LOO} have similar performances; their RMSEs are monotonically (almost linearly) decreasing. This is not the case of MSE and EIGF. The MSE method does not perform well in dimensions 5 and 6. It seems that MSE selects many samples on the boundary of the input space where the GP predictive variance is high. The EIGF method has the best performance only on the Friedman function (f_3) and has the lowest accuracy in approximating other functions, especially f_4 .

4.3 Real-world problems

We also tested our method on two real-world problems which are the 6-dimensional *output transformerless (OTL) circuit* and 7-dimensional *piston simulation* functions [4]. The former (f_{OTL}) returns the midpoint voltage of a transformerless circuit and the latter (f_{piston}) measures the cycle time that a piston takes to complete one cycle within a cylinder. The analytical expressions of f_{OTL} and f_{piston} and their design spaces are given in Appendix B. Figure 8 illustrates the results of comparing our proposed method with MSE, EIGF and LHS design. The experimental setup is the same as explained in Section 4.1. The sequential (black) and batch (orange) ESE_{LOO} have again similar performances and are the best sampling approaches on the piston simulation function. The RMSE criterion associated with ESE_{LOO} (both sequential and batch) reduces steadily on the two problems as is observed in Figure 7. The MSE approach does not work well especially after almost $10 \times d$ function evaluations. It seems that MSE is not a good sampling strategy when the dimensionality of the problem is larger than 5. While EIGF has the best performance on the OTL circuit problem, there is no improvement in the prediction accuracy of the emulator after $10 \times d$ evaluations of the piston simulation function.

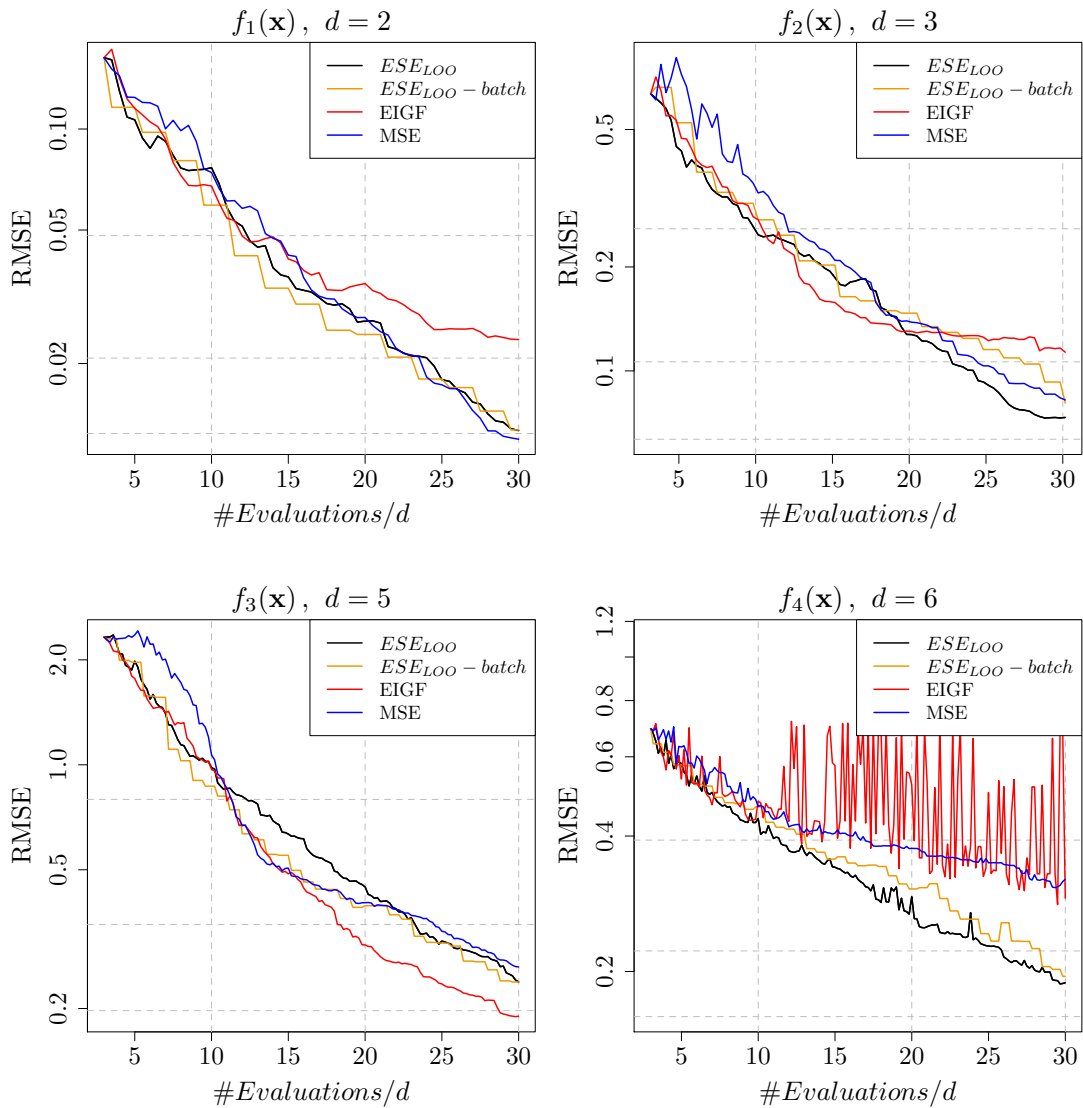


Figure 7: The median of ten RMSEs of our proposed approach ESE_{LOO} : sequential (black) and batch with $q = 4$ (orange), EIGF (red) and MSE (blue). Ten different initial DoEs of size $3d$ are considered for each function; every method produces ten predictions based on them. The total budget is $30d$. The dashed grey lines show the median of RMSEs based on one-shot space-filling designs of sizes (from top to bottom): $10d$, $20d$ and $30d$, respectively. The y -axis is on logarithmic scale.

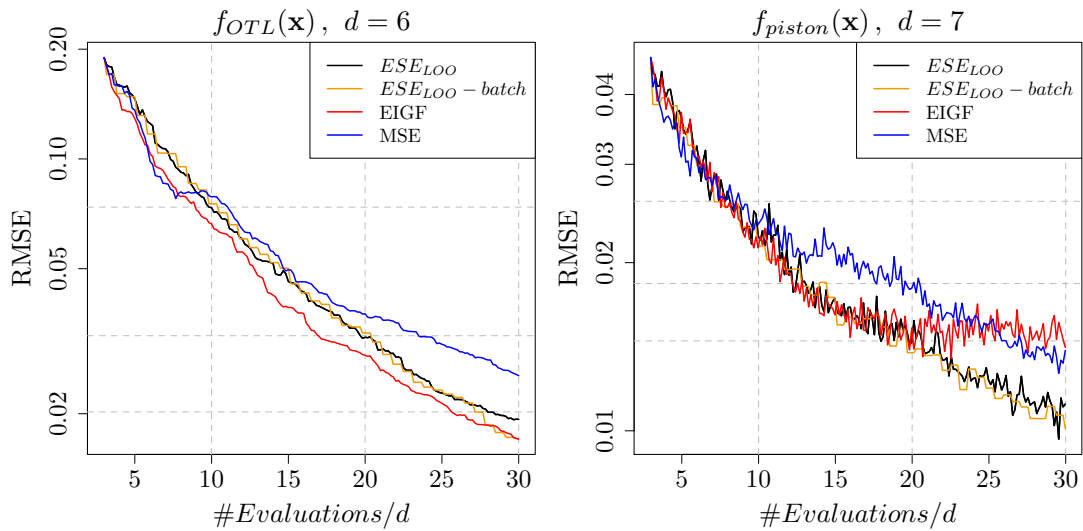


Figure 8: The median of ten RMSEs of our proposed approach ESE_{LOO} : sequential (black) and batch with $q = 4$ (orange), EIGF (red) and MSE (blue). The dashed grey lines show the median of RMSEs based on one-shot space-filling designs of sizes (from top to bottom): $10d, 20d$ and $30d$, respectively.

5 Conclusion

This paper deals with the problem of extending an initial experiment sequentially for training GP models. This is an important issue in the context of emulating computationally expensive computer codes where the goal is to approximate the underlying function with a minimum number of evaluation. An adaptive sampling scheme is presented based on the expected squared leave-one-out error, ESE_{LOO} , which is used to identify “good” locations for future function evaluations. Since ESE_{LOO} is only known at the design points, another GP model is applied to approximate it at unobserved sites. Then, the pseudo expected improvement criterion is employed to find the location of maximum of ESE_{LOO} as the most promising point to improve the emulator. Once the new sample is chosen, it is added to the existing designs and the procedure is repeated until a stopping criterion is met. The proposed method can be easily promoted to a batch mode where at each iteration a set of input points is selected for evaluation. This can save the user time if parallel computing is available. Several test functions are used to test the capability of our method and it is compared with two other methods relying on the mean squared error and expected improvement for global fit criteria. The results show that the proposed adaptive sampling approach is promising.

Acknowledgements

The authors gratefully acknowledge the financial support of the EPSRC via grant EP/N014391/1.

Appendix A Test function expressions

The analytic expressions of four test functions used in our experiments are given below.

1. $f_1(\mathbf{x}) = 0.75 \exp\left(-\frac{(9x_1-2)^2}{4} - \frac{(9x_2-2)^2}{4}\right) + 0.75 \exp\left(-\frac{(9x_1+1)^2}{49} - \frac{9x_2+1}{10}\right) + 0.5 \exp\left(-\frac{(9x_1-7)^2}{4} - \frac{(9x_2-3)^2}{4}\right) - 0.2 \exp(-(9x_1 - 4)^2 - (9x_2 - 7)^2).$

2. $f_2(\mathbf{x}) = -\sum_{i=1}^4 \alpha_i \exp\left(\sum_{j=1}^3 \mathbf{A}_{ij} (x_j - \mathbf{P}_{ij})^2\right)$ where $\alpha = (1, 1.2, 3, 3.2)^\top$,

$$\mathbf{A} = \begin{bmatrix} 3 & 10 & 30 \\ 0.1 & 10 & 35 \\ 3 & 10 & 30 \\ 0.1 & 10 & 35 \end{bmatrix}, \quad \mathbf{P} = 10^{-4} \begin{bmatrix} 3689 & 1170 & 2673 \\ 4699 & 4387 & 7470 \\ 1091 & 8732 & 5547 \\ 381 & 5743 & 8828 \end{bmatrix}.$$

3. $f_3(\mathbf{x}) = 10 \sin(\pi x_1 x_2) + 20(x_3 - 0.5)^2 + 10x_4 + 5x_5.$

4. $f_4(\mathbf{x}) = \exp(\sin([0.9(x_1 + 0.48)])^{10}) + x_2 x_3 + x_4.$

Appendix B Real-world function expressions

OTL circuit function The function f_{OTL} is defined as

$$f_{OTL}(\mathbf{x}) = \frac{(V_{b1} + 0.74)\beta(R_{c2} + 9)}{\beta(R_{c2} + 9) + R_f} + \frac{11.35R_f}{\beta(R_{c2} + 9) + R_f} + \frac{0.74R_f\beta(R_{c2} + 9)}{(\beta(R_{c2} + 9) + R_f)R_{c1}},$$

where $V_{b1} = \frac{12R_{b2}}{R_{b1} + R_{b2}}$. The input variables of f_{OTL} are:

- $R_{b1} \in [50, 150]$ is the resistance b_1 (K-Ohms)
- $R_{b2} \in [25, 70]$ is the resistance b_2 (K-Ohms)
- $R_f \in [0.5, 3]$ is the resistance f (K-Ohms)
- $R_{c1} \in [1.2, 2.5]$ is the resistance c_1 (K-Ohms)
- $R_{c2} \in [0.25, 1.2]$ is the resistance c_2 (K-Ohms)
- $\beta \in [50, 300]$ is the current gain c_1 (Amperes).

Piston simulation function The function f_{piston} is defined as

$$f_{piston}(\mathbf{x}) = 2\pi \sqrt{\frac{M}{k + S^2 \frac{P_0 V_0 T_a}{T_0 V^2}}}, \quad \text{where } V = \frac{S}{2k} \left(\sqrt{A^2 + 4k \frac{P_0 V_0}{T_0} T_a} - A \right),$$

$$A = P_0 S + 19.62M - \frac{kV_0}{S}.$$

The input variables of f_{piston} are:

- $M \in [30, 60]$ is the piston weight (kg)
- $S \in [0.005, 0.020]$ is the piston surface area (m^2)
- $V_0 \in [0.002, 0.010]$ is the initial gas volume (m^3)
- $k \in [1000, 5000]$ is the spring coefficient (N/m)
- $P_0 \in [90000, 110000]$ is the atmospheric pressure (N/m^2)
- $T_a \in [290, 296]$ is the ambient temperature (K)
- $T_0 \in [340, 360]$ is the filling gas temperature (K).

References

- [1] V. Aute, K. Saleh, O. Abdelaziz, S. Azarm, and R. Radermacher. Cross-validation based single response adaptive design of experiments for kriging metamodeling of deterministic computer simulations. *Structural and Multidisciplinary Optimization*, 48(3):581–605, 2013.
- [2] Gregory A. Banyay, Michael D. Shields, and John C. Brigham. Efficient global sensitivity analysis for flow-induced vibration of a nuclear reactor assembly using kriging surrogates. *Nuclear Engineering and Design*, 341:1 – 15, 2019.
- [3] J. Beck and S. Guillas. Sequential design with mutual information for computer experiments (MICE): Emulation of a tsunami model. *SIAM/ASA Journal on Uncertainty Quantification*, 4(1):739–766, 2016.
- [4] Einat Neumann Ben-Ari and David M. Steinberg. Modeling data from computer experiments: An empirical comparison of kriging with mars and projection pursuit regression. *Quality Engineering*, 19(4):327–338, 2007.
- [5] M. Ben Salem, O. Roustant, F. Gamboa, and L. Tomaso. Universal prediction distribution for surrogate models. *SIAM/ASA Journal on Uncertainty Quantification*, 5(1):1086–1109, 2017.
- [6] G. E. P. Box and J. S. Hunter. The 2^{k-p} fractional factorial designs part ii. *Technometrics*, 3(4):449–458, 1961.
- [7] Eric Brochu, Vlad M. Cora, and Nando de Freitas. A tutorial on Bayesian optimization of expensive cost functions, with application to active user modeling and hierarchical reinforcement learning. *CoRR*, abs/1012.2599, 2010.
- [8] William F Caselton and James V Zidek. Optimal monitoring network designs. *Statistics and Probability Letters*, 2(4):223–227, 1984.
- [9] Olivier Dubrule. Cross validation of kriging in a unique neighborhood. *Journal of the International Association for Mathematical Geology*, 15(6):687–699, 1983.
- [10] Delphine Dupuy, Céline Helbert, and Jessica Franco. DiceDesign and DiceEval: two R packages for design and analysis of computer experiments. *Journal of Statistical Software*, 65(11):1–38, 2015.
- [11] Jerome H. Friedman. Multivariate adaptive regression splines. *The Annals of Statistics*, 19(1):1–67, 1991.
- [12] Sushant S. Garud, Iftekhar A. Karimi, and Markus Kraft. Design of computer experiments: A review. *Computers & Chemical Engineering*, 106:71 – 95, 2017. ESCAPE-26.

- [13] Andrew Gelman, John Carlin, Hal Stern, David Dunson, Aki Vehtari, and Donald Rubin. Bayesian Data Analysis, Third Edition (Chapman & Hall/CRC Texts in Statistical Science). Hardcover, 2013.
- [14] Robert B. Gramacy and Herbert K. H. Lee. Adaptive design and analysis of super-computer experiments. *Technometrics*, 51(2):130–145, 2009.
- [15] Ben Haaland and Peter Z. G. Qian. Accurate emulators for large-scale computer experiments. *The Annals of Statistics*, 39(6):2974–3002, 2011.
- [16] Momin Jamil and Xin-She Yang. A literature survey of benchmark functions for global optimization problems. *International Journal of Mathematical Modelling and Numerical Optimisation*, 4(2):150–194, 2013.
- [17] Ruichen Jin, Wei Chen, and Agus Sudjianto. On sequential sampling for global meta-modeling in engineering design. In *Design Engineering Technical Conferences And Computers and Information in Engineering*, volume 2, pages 539–548, 2002.
- [18] Donald R. Jones. A taxonomy of global optimization methods based on response surfaces. *Journal of Global Optimization*, 21(4):345–383, Dec 2001.
- [19] Donald R. Jones, Matthias Schonlau, and William J. Welch. Efficient global optimization of expensive black-box functions. *Journal of Global Optimization*, 13(4):455–492, 1998.
- [20] V. Roshan Joseph. Space-filling designs for computer experiments: A review. *Quality Engineering*, 28(1):28–35, 2016.
- [21] Crombecq Karel, Dirk Gorissen, Dirk Deschrijver, and Tom Dhaene. A novel hybrid sequential design strategy for global surrogate modeling of computer experiments. *SIAM Journal on Scientific Computing*, 33(4):1948–1974, 2011.
- [22] J.R. Koehler and A.B. Owen. Computer experiments. In *Design and Analysis of Experiments*, volume 13 of *Handbook of Statistics*, pages 261 – 308. Elsevier, 1996.
- [23] Andreas Krause, Ajit Singh, and Carlos Guestrin. Near-optimal sensor placements in Gaussian processes: Theory, efficient algorithms and empirical studies. *Journal of Machine Learning Research*, 9:235–284, February 2008.
- [24] Chen Quin Lam. *Sequential adaptive designs in computer experiments for response surface model fit*. PhD thesis, Columbus, OH, USA, 2008. AAI3321369.
- [25] Loic Le Gratiet and Claire Cannamela. Kriging-based sequential design strategies using fast cross-validation techniques with extensions to multi-fidelity computer codes. *arXiv e-prints*, page arXiv:1210.6187, 2012.

- [26] Genzi Li, Vikrant Aute, and Shapour Azarm. An accumulative error based adaptive design of experiments for offline metamodeling. *Structural and Multidisciplinary Optimization*, 40(1):137–157, 2009.
- [27] D. Liu, A. Litvinenko, C. Schillings, and V. Schulz. Quantification of airfoil geometry-induced aerodynamic uncertainties—comparison of approaches. *SIAM/ASA Journal on Uncertainty Quantification*, 5(1):334–352, 2017.
- [28] Haitao Liu, Yew-Soon Ong, and Jianfei Cai. A survey of adaptive sampling for global metamodeling in support of simulation-based complex engineering design. *Structural and Multidisciplinary Optimization*, 57(1):393–416, 2018.
- [29] Haitao Liu, Shengli Xu, Ying Ma, Xudong Chen, and Xiaofang Wang. An adaptive Bayesian sequential sampling approach for global metamodeling. *Journal of Mechanical Design*, 138(1), 2015.
- [30] Jay Martin and Timothy Simpson. Use of adaptive metamodeling for design optimization. In *9th AIAA/ISSMO Symposium on Multidisciplinary Analysis and Optimization*, pages 1–9, 2002.
- [31] M. D. McKay, R. J. Beckman, and W. J. Conover. A comparison of three methods for selecting values of input variables in the analysis of output from a computer code. *Technometrics*, 21(2):239–245, 1979.
- [32] Hossein Mohammadi. *Kriging-based black-box global optimization: analysis and new algorithms*. PhD thesis, École Nationale Supérieure des Mines de Saint-Étienne, France, 2016.
- [33] Radford M. Neal. Regression and classification using Gaussian process priors. pages 475–501. *Bayesian Statistics 6*, Oxford University Press, 1998.
- [34] Art B. Owen. Orthogonal arrays for computer experiments, integration and visualization. *Statistica Sinica*, 2(2):439–452, 1992.
- [35] V. Picheny, D. Ginsbourger, O. Roustant, R. T. Haftka, and N. H. Kim. Adaptive designs of experiments for accurate approximation of a target region. *Journal of Mechanical Design*, 132(7):1–9, 2010.
- [36] W. Ponweiser, T. Wagner, and M. Vincze. Clustered multiple generalized expected improvement: A novel infill sampling criterion for surrogate models. In *2008 IEEE Congress on Evolutionary Computation (IEEE World Congress on Computational Intelligence)*, pages 3515–3522, 2008.
- [37] Luc Pronzato and Werner G. Müller. Design of computer experiments: space filling and beyond. *Statistics and Computing*, 22(3):681–701, 2012.

- [38] Carl Edward Rasmussen and Christopher K. I. Williams. *Gaussian processes for machine learning (adaptive computation and machine learning)*. The MIT Press, 2005.
- [39] Olivier Roustant, David Ginsbourger, and Yves Deville. DiceKriging, DiceOptim: Two R packages for the analysis of computer experiments by kriging-based metamodeling and optimization. *Journal of Statistical Software*, 51(1):1–55, 2012.
- [40] Jerome Sacks, William J. Welch, Toby J. Mitchell, and Henry P. Wynn. Design and analysis of computer experiments. *Statistical Science*, 4(4):409–423, 1989.
- [41] T. J. Santner, Williams B., and Notz W. *The design and analysis of computer experiments*. Springer-Verlag, 2003.
- [42] Matthias Schonlau. *Computer experiments and global optimization*. PhD thesis, University of Waterloo, 1997.
- [43] Razi Sheikholeslami and Saman Razavi. Progressive latin hypercube sampling: an efficient approach for robust sampling-based analysis of environmental models. *Environmental Modelling & Software*, 93:109 – 126, 2017.
- [44] M. C. Shewry and H. P. Wynn. Maximum entropy sampling. *Journal of Applied Statistics*, 14(2):165–170, 1987.
- [45] T.W. Simpson, J.D. Poplinski, P. N. Koch, and J.K. Allen. Metamodels for computer-based engineering design: Survey and recommendations. *Engineering with Computers*, 17(2):129–150, 2001.
- [46] Ian Vernon, Junli Liu, Michael Goldstein, James Rowe, Jen Topping, and Keith Lindsey. Bayesian uncertainty analysis for complex systems biology models: emulation, global parameter searches and evaluation of gene functions. *BMC Systems Biology*, 12(1):1, 2018.
- [47] Victoria Volodina and Daniel Williamson. Diagnostics-driven nonstationary emulators using kernel mixtures. *SIAM/ASA Journal on Uncertainty Quantification*, 8(1):1–26, 2020.
- [48] Daniel Williamson. Exploratory ensemble designs for environmental models using k-extended Latin Hypercubes. *Environmetrics*, 26(4):268–283, 2015.
- [49] Dawei Zhan, Jiachang Qian, and Yuansheng Cheng. Pseudo expected improvement criterion for parallel EGO algorithm. *Journal of Global Optimization*, 68(3):641–662, 2017.